TO APPEAR IN THE ASTROPHYSICAL JOURNAL LETTERS
Preprint typeset using LaTeX style emulateapj v. 14/09/00

arXiv:astro-ph/0207540v2 25 Sep 2002

THE LIKELY NEAR-INFRARED COUNTERPART TO THE ANOMALOUS X-RAY PULSAR 1E 1048.1–5937[1]

ZHONGXIANG WANG[2] AND DEEPTO CHAKRABARTY[2,3]
Department of Physics and Center for Space Research, Massachusetts Institute of Technology, Cambridge, MA 02139;
wangzx@space.mit.edu, deepto@space.mit.edu
To appear in the Astrophysical Journal Letters

ABSTRACT

We report our discovery of the likely near-infrared counterpart to the anomalous X-ray pulsar (AXP) 1E 1048.1–5937, using observations from the 6.5 m Baade (Magellan I) telescope in Chile. We derived a precise position for the X-ray source using archival data from the *Chandra X-Ray Observatory*. This position is inconsistent with a position reported earlier from *XMM-Newton*, but we show that the originally reported *XMM-Newton* position suffered from attitude reconstruction problems. Only two of the infrared objects in a $17''\times17''$ field containing the target have unusual colors, and one of these has colors consistent with those of the identified counterparts of two other AXPs. The latter object is also the only source detected within the $0\farcs6$ *Chandra* error circle, and we identify it as the counterpart to 1E 1048.1–5937. This is the first AXP counterpart detected in multiple infrared bands, with magnitudes J=21.7(3), H=20.8(3), and K=19.4(3). There is marginal evidence for spectral flattening at longer wavelengths.

Subject headings: pulsars: individual (1E 1048.1–5937) — stars: neutron

1. INTRODUCTION

The anomalous X-ray pulsars (AXPs) are a small group of neutron stars with spin periods falling in a narrow range (6–12 s), very soft X-ray spectra, and with no evidence of binary companions (see Mereghetti et al. 2002 for a recent review). Their X-ray luminosities greatly exceed the power available from spin-down of the pulsars. These objects are thus believed to be isolated neutron stars either having extremely strong ($\sim 10^{14}$ G) surface magnetic fields ("magnetars") or accreting from a residual accretion disk. X-ray bursts detected from the AXPs 1E 1048.1–5937 (Gavriil, Kaspi, & Woods 2002) and 1E 2259+586 (Kaspi & Gavriil 2002) have strengthened an already suspected connection to the soft gamma-ray repeaters (SGRs). The recent identification of optical/infrared counterparts to the AXPs 4U 0142+61 (Hulleman, van Kerkwijk, & Kulkarni 2000) and 1E 2259+586 (Hulleman et al. 2001) and the discovery of optical pulsations from 4U 0142+61 (Kern & Martin 2002) favor the magnetar scenario for these objects. In this paper, we report on the detection of a third AXP counterpart, and the first measurement of infrared colors for one of these objects.

The AXP 1E 1048.1–5937 (l=288.°3, b=–0.°5) was discovered serendipitously in 1979 during an *Einstein* observation of the Carina Nebula (Seward, Charles, & Smale 1986). It has since been extensively observed by a series of X-ray missions including *EXOSAT* (Seward et al. 1986), *Ginga* (Corbet & Day 1990), *ROSAT* (Mereghetti 1995), *ASCA* (Corbet & Mihara 1997; Paul et al. 2000), *RXTE* (Mereghetti, Israel, & Stella 1998; Baykal et al. 2000; Kaspi et al. 2001; Gavriil et al. 2002), and *XMM-Newton* (Tiengo et al. 2002). These observations establish the source as a 6.4 s pulsar that is spinning down, with an absorbed power-law + blackbody X-ray spectrum and occasional SGR-like bursts. The high column density to the source indicates that it lies behind the Carina Nebula, setting a lower limit on its distance of $d \gtrsim 2.8$ kpc (Seward et al. 1986; Özel, Psaltis, & Kaspi 2001). Previous searches for an optical counterpart have been unsuccessful (Seward et al. 1986; Mereghetti, Caraveo, & Bignami 1992) with the resultant limiting magnitudes $BVR \gtrsim 24.3$ (Israel, Mereghetti, & Stella 2001).

2. OPTICAL AND INFRARED OBSERVATIONS

We obtained optical images of the field around 1E 1048.1–5937 on 2001 March 24 using the Raymond and Beverly Sackler Magellan Instant Camera (MagIC) at the west f/11 Nasmyth focus of the 6.5 m Baade (Magellan I) telescope at Las Campanas Observatory in Chile. MagIC is a 2048×2048 SITe CCD with a $0\farcs069$ pixel^{-1} plate scale and a $142''$ field of view. Our observations were made using the Sloan filter set (Fukugita et al. 1996). We obtained 10 min exposures in the r' and i' bands. The seeing during the night was around $1''$. The limiting magnitudes (3σ) reached were r' = 24.8 and i' = 24.4. Photometric standards GD 108 and RU 152F were observed at various airmasses for calibration (Landolt 1992)

We also obtained JHK_s near-infrared images of the 1E 1048.1–5937 field on 2002 February 25 using the Ohio State Infrared Imager/Spectrometer (OSIRIS; Depoy et al. 1993) at the f/14 tip-tilt focus of the 4 m Blanco telescope at the Cerro Tololo Inter-American Observatory (CTIO) in Chile. The detector in OSIRIS was a Rockwell HAWAII HgCdTe 1024×1024 array. We used the OSIRIS f/7 camera, which had a $0\farcs161$ pixel^{-1} plate scale and a $93''$ field of view. For each wavelength band, we obtained nine images in a 3×3 grid with offsets of about $10''$ to allow for correction of the rapidly varying infrared sky background and to minimize the effect of bad

[1] Based in part on observations from the 6.5 m Baade telescope operated by the Observatories of the Carnegie Institution of Washington for the Magellan Consortium, a collaboration between the Carnegie Observatories, the University of Arizona, Harvard University, the University of Michigan, and the Massachusetts Institute of Technology.

[2] Visiting astronomer, Cerro Tololo Inter-American Observatory, National Optical Astronomy Observatories, operated by the Association of Universities for Research in Astronomy under contract to the National Science Foundation.

[3] Alfred P. Sloan Research Fellow.

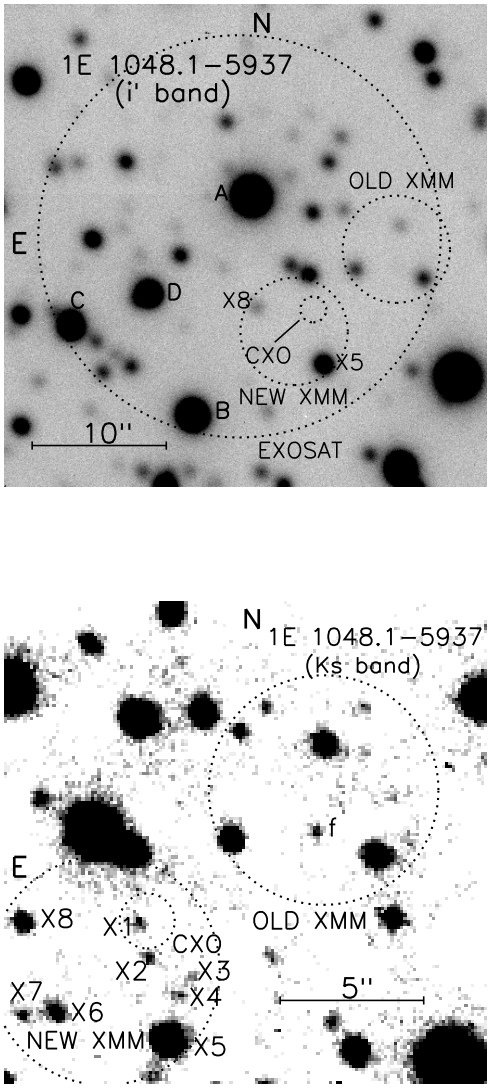

FIG. 1.— Optical and near-infrared images of the 1E 1048.1–5937 field. *Top panel:* i'-band image. *Bottom panel:* K_s-band Magellan image. On both images the *Chandra* (CXO) and *XMM-Newton* (old and new) error circles are shown. Also shown is the 15″ *EXOSAT* error circle on the optical image. The candidates *X1–X2* are discussed in §4. Objects *A*, *B*, *C*, and *D* in the optical image were studied by Mereghetti et al. (1992). Our proposed counterpart is object *X1*.

pixels. These individual images were shifted and combined in the course of the data reduction. Our total exposure in each band was 4.5 min in J, 9 min in H, and 4.5 min in K_s. During the night the seeing was good, varying from 0.″8 to 1.″2. The limiting magnitudes (3σ) reached were $J = 21.3$, $H = 20.2$, and $K_s = 19.3$. The near-IR photometric standards 9136 and LHS 2397a of Persson et al. (1998) were observed for calibration.

We obtained deeper JHK_s images of the target field on 2002 April 8 with the "Classic Cam" near-infrared imager (Persson et al. 1992, 2001) at the west f/11 Nasmyth focus on the 6.5 m Baade telescope. The detector was a Rockwell NICMOS3 HgCdTe 256×256 array. We selected the camera in its low-resolution mode, with a 0.″112 pixel^{-1} plate scale and a 29″ field of view. The total exposure for 1E 1048.1–5937 in each band was 10.5 min in J, 18 min in H, and 15 min in K_s. The same dithering and data reduction scheme was employed as with the CTIO observations. The conditions were good, with the seeing around 0.″8. The limiting magnitudes (3σ) reached were $J = 21.7$, $H = 20.8$, and $K_s = 19.7$. The same IR standards were used as in the CTIO observations.

We used the IRAF data analysis package to reduce our data, including the DAOPHOT routines for crowded field photometry.

3. X-RAY POSITION AND ASTROMETRY

We derived the position of 1E 1048.1–5937 using data from the *Chandra X-Ray Observatory* public data archive. The source was observed with the imaging detector of the *Chandra* High-Resolution Camera (HRC-I; Zombeck et al. 1995) on 2001 July 4 for 9.87 ks. We analyzed these data using the CIAO v2.2 data analysis package.[4] To maximize the absolute positional accuracy of the data, we used the CIAO thread (processing recipe) `fix_offset` to check for systematic aspect offsets and apply the latest alignment file (2002 May 2) as necessary. Using the CIAO tool `celldetect`, we obtained the following source position: R.A. = $10^{\rm h}50^{\rm m}07\overset{\rm s}{.}14$ and Decl. = –59°53′21.″4 (equinox J2000.0), with an error radius of 0.″6 (90% confidence) dominated by the spacecraft attitude uncertainty. No other sources were detected in the *Chandra* image.

We note that our *Chandra* position differs significantly (7.″6) from the position reported by Tiengo et al. (2002) from *XMM-Newton* observations: R.A. = $10^{\rm h}50^{\rm m}06\overset{\rm s}{.}3$, Decl. = –59°53′17″ (equinox J2000.0), with an error radius of 4″. We reanalyzed these data and obtained a position consistent with that of Tiengo et al. (2002). However, an examination of the *XMM-Newton* spacecraft attitude history during this observation indicates an unusually large and oscillating offset between the commanded and attitude-reconstructed viewing directions, with a mean value of 10.″5 and an amplitude of 2″. In consulting with the *XMM-Newton* User Support Group, we learned that such offsets usually (but not always) reflect problems with the attitude measurement accuracy rather than a pointing error, resulting in an erroneous reconstruction of the spacecraft attitude and the source coordinates (M. Santos-Lleo 2002, private communication). We were later informed by the *XMM-Newton* project that they have revised their attitude determination algorithm, placing less emphasis on the satellite pitch angle as determined from the fine sun sensor in the unusual case of tracking on a single guide star, as in this observation (F. Jansen 2002, private communication). This has led to a revised *XMM-Newton* position: R.A. = $10^{\rm h}50^{\rm m}07\overset{\rm s}{.}31$, Decl. = –59°53′23.″1, equinox J2000.0, error radius 4″. This is consistent with the *Chandra* position. We show both the original and the revised positions in Figure 1. We thus disregard the *XMM-Newton* position reported by Tiengo et al. (2002).

An astrometric solution for the optical images was derived by matching about 20 unsaturated field stars with the USNO-A2.0 catalog of astrometric standards (Monet et al. 1998). Since the field of view of our infrared images is too small to allow a direct tie to the USNO-A2.0 system, we derived an astrometric solution for these images indirectly by matching stars with our optical images. The total nominal uncertainty for locating the *Chandra* source position on our optical/infrared images is 1″

[4] See http://asc.harvard.edu/ciao/

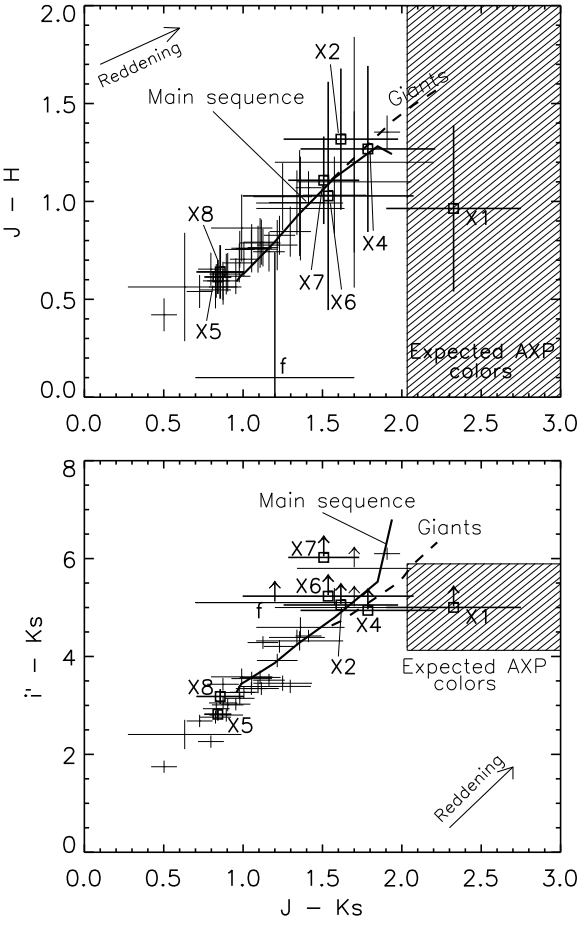

FIG. 2.— Color-color diagrams for the objects in the field of 1E 1048.1–5937. The dark squares indicate the candidates discussed in §4 and the light crosses indicate other field stars. The direction of increasing reddening is indicated by the arrow. The dark solid and dashed lines indicate the expected colors for main sequence and giant stars, respectively, with a reddening of $A_V = 5.8$. The shaded region indicates the expected counterpart colors given the properties of the two other known AXP counterparts. Only our proposed counterpart (*X1*) lies in this region; it is also the only detected source in the *Chandra* error circle.

(90% confidence), which includes the systematic uncertainty of the USNO-A2.0 catalog (0.″25; Monet et al. 1998), the transformation uncertainty between the optical image and the USNO-A2.0 catalog (0.″4), and the uncertainty of *Chandra* observation. For the *XMM-Newton* position, the quoted 4″ uncertainty dominates. In Figure 1, we show our i' and K_s images of the field of 1E 1048.1–5937 with the error circles of both *Chandra* and *XMM-Newton* plotted.

4. RESULTS

As seen in the top panel of Figure 1, no objects were detected within the *Chandra* error circle in our optical images, although two objects (labeled *X5* and *X8*) were detected within the revised *XMM-Newton* error circle. Also indicated in that panel are the candidates (*A*, *B*, *C*, and *D*) previously studied by Mereghetti et al. (1992). In the bottom panel of Figure 1, we detected one object (*X1*) within the *Chandra* error circle in our deep infrared images and another (*X2*) just outside. In addition,

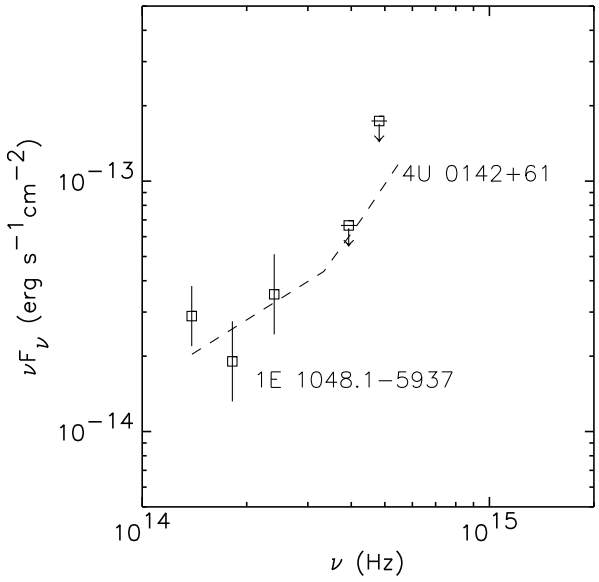

FIG. 3.— Dereddened flux from object *X1*, the counterpart to 1E 1048.1–5937. For comparison, the dashed line indicates the interpolated dereddened flux from AXP 4U 0142+61 (Hulleman et al. 2000; Hulleman 2002).

we detected six other objects (labeled as *X3*–*X8*) within the revised *XMM-Newton* error circle. Object *X3* was detected only in the K_s band; since we cannot derive colors for this object, it is excluded from further consideration below. The faint objects *X3*, *X4*, and *X1* were not detected in our CTIO JHK_s observations, which were not as deep as the Magellan observations. The positions and optical/infrared magnitudes of our candidates are summarized in Table 1.

Figure 2 shows color-color diagrams for our seven candidates as well as all other field stars in our Classic Cam images. We note that the inferred hydrogen column density to 1E 1048.1–5937, $N_{\rm H} = 1.04(8) \times 10^{22}$ cm^{-2} (Tiengo et al. 2001), implies a visual extinction of $A_V \simeq 5.8$ for a typical dust-to-gas ratio (Predehl & Schmitt 1995). For comparison in Figure 2, we also show the expected colors for main sequence and giant stars (Bessell & Brett 1988; Cox 2000) reddened by $A_V = 5.8$ (Rieke & Lebofsky 1985; Fan 1999). The reddening vector lies roughly parallel to this locus of points. Most of our candidates (as well as the other field stars) have colors consistent with those of normal stars. However, two objects, *f* and *X*1, stand out with unusual colors. Assuming that the counterpart of 1E 1048.1–5937 is similar to those of the AXPs 4U 0142+61 ($V = 25.62 \pm 0.08$, $R = 24.99 \pm 0.07$, $I = 23.84 \pm 0.06$, $K = 19.6$, $A_V = 5.4$; Hulleman et al. 2000; Hulleman 2002) and 1E 2259+586 ($R > 26.4$, $I > 25.6$, $J > 23.8$, $K_s = 21.7 \pm 0.2$, $A_V = 5.2$; Hulleman et al. 2001), we have also indicated in Figure 2 the region of color-color space in which we would expect to find the counterpart. Only candidate *X1* has colors consistent with these predictions. We further note that *X1* is the only object detected within the *Chandra* error circle. We therefore conclude that this object is the near-infrared counterpart to 1E 1048.1–5937.

5. SUMMARY

We have identified the likely near-infrared counterpart to 1E 1048.1–5937, on the basis of coincidence with the *Chandra* X-ray source position, unusual colors, and similarity to the

TABLE 1

ASTROMETRY AND PHOTOMETRY OF CANDIDATE COUNTERPARTS

ID	R.A. (J2000)	Decl. (J2000)	r'	i'	J	H	K_s
X1[a]	$10^h50^m07^s.13$	$-59°53'21.''3$	>24.8	> 24.4	21.7(3)	20.8(3)	19.4(3)
X2	$10^h50^m07^s.09$	$-59°53'22.''5$	>24.8	> 24.4	21.0(2)	19.7(3)	19.3(3)
X3	$10^h50^m06^s.89$	$-59°53'23.''2$	>24.8	> 24.4	>21.7	>20.8	20.3(4)
X4	$10^h50^m06^s.94$	$-59°53'23.''8$	>24.8	> 24.4	21.2(3)	20.0(3)	19.5(3)
X5	$10^h50^m07^s.00$	$-59°53'25.''5$	19.8(1)	19.0(1)	17.04(2)	16.42(8)	16.20(8)
X6	$10^h50^m07^s.09$	$-59°53'24.''4$	>24.8	> 24.4	19.9(2)	18.8(1)	18.4(1)
X7	$10^h50^m07^s.67$	$-59°53'24.''4$	>24.8	> 24.4	20.7(5)	19.7(3)	19.2(2)
X8	$10^h50^m07^s.66$	$-59°53'21.''2$	22.3(1)	21.3(1)	19.0(1)	18.3(1)	18.1(1)
f	$10^h50^m06^s.29$	$-59°53'18.''2$	>24.8	> 24.4	20.5(4)	20.4(5)	19.3(3)
A	$10^h50^m07^s.71$	$-59°53'12.''9$	16.5(1)	16.2(1)	14.875(6)	14.45(8)	14.37(8)
B	$10^h50^m08^s.31$	$-59°53'29.''3$	17.6(1)	17.0(1)	15.170(7)	14.69(8)	14.49(8)
C	$10^h50^m09^s.52$	$-59°53'22.''6$	18.5(1)	17.8(1)	14.783(7)	13.71(8)	13.37(8)
D	$10^h50^m08^s.74$	$-59°53'20.''1$	19.1(1)	17.8(1)	16.46(3)	15.90(9)	15.65(9)

[a]Proposed counterpart to 1E 1048.1–5937.

two other known AXP counterparts. We note, however, that this conclusion relies strongly on our i' non-detection. A sufficiently faint i' magnitude could push this candidate out of the expected AXP region in the bottom panel of Figure 2. This is the first AXP counterpart with infrared detections in more than one band, allowing the intrinsic infrared colors to be inferred. Assuming $A_V = 5.8$ as determined in §4, the dereddened infrared magnitudes of the counterpart are $J_0 = 20.1$, $H_0 = 20.0$, and $K_{s0} = 18.8$. We plot these magnitudes and limits in Figure 3. For comparison, we plot the inferred spectral shape of the 4U 0142+61 counterpart (Hulleman et al. 2000; Hulleman 2002). While there is marginal evidence for a spectral flattening or even a turnover at the K_s band, the data are also consistent with a flat νF_ν infrared spectrum at the 1σ level. We note that there is clear evidence for spectral flattening in the infrared in the spectrum of 4U 0142+61 (Hulleman 2002). It would thus be of great interest to search for emission at longer wavelengths to constrain the spectral shape of AXPs further. While there has been relatively little theoretical work presented on the expected AXP optical/infrared emission in the magnetar scenario, we note that models involving X-ray illumination of a "fallback" accretion disk predict a spectral turnover leading to strong emission in the infrared and submillimeter bands (e.g., Chatterjee, Hernquist, & Narayan 2000; Perna, Hernquist, & Narayan 2000).

We thank Paul Schechter for obtaining the 2001 March Magellan data for us; Jim Elliot, Mauricio Navarrete, Hernán Nuñez, Patricio Jones, Geraldo Valladanes, and the LCO staff for their help during the 2002 April Magellan run; Eric Persson for advice on obtaining and analyzing Classic Cam data; and Nicole van der Bliek, Robert Blum, Angel Guerra, Sergio Pizarro, and the CTIO staff for their assistance during our CTIO run. We also thank Scott Burles for useful discussions, Adrienne Juett for assistance in analyzing the X-ray data, and Maria Santos-Lleo of the *XMM-Newton* User Support Group for guidance in understanding the *XMM-Newton* aspect determination problem. Finally, we thank the referee for a careful review of our paper.

REFERENCES

Baykal, A., Strohmayer, T., Swank, J., Alpar, M. A., & Stark, M. J. 2000, MNRAS, 319, 205
Bessell, M. S. & Brett, J. M. 1988, PASP, 100, 1134
Chatterjee, P., Hernquist, L., & Narayan, R. 2000, ApJ, 534, 373
Corbet, R. H. D. & Day, C. S. R. 1990, MNRAS, 243, 553
Corbet, R. H. D. & Mihara, T. 1997, ApJ, 475, L127
Cox, A. N. 2000, Allen's Astrophysical Quantities, 4th ed. (New York: Springer)
Depoy, D., Atwood, B., Byard, P. L., Frogel, J., & O'Brien, T. P. 1993, Proc. SPIE, 1946, 667
Fan, X. 1999, AJ, 117, 2528
Fukugita, M. et al. 1996, AJ, 111, 1748
Gavriil, F. P., Kaspi, V. M., Woods, P. M. 2002, Nature, in press
Hulleman, F. 2002, in Neutron Stars in Supernova Remnants, ed. P. O. Slane and B. M. Gaensler (San Francisco: ASP), in press (astro-ph/0111561)
Hulleman, F., Tennant, A. F., van Kerkwijk, M. H., Kulkarni, S. R., Kouveliotou, C., & Patel, S. K. 2001, ApJ, 563, L49
Hulleman, F., van Kerkwijk, M. H., & Kulkarni, S. R. 2000, Nature, 408, 689
Israel G., Mereghetti, S., & Stella, L. 2001, in Soft Gamma Repeaters: The Rome 2000 Mini-workshop, eds. M. Feroci and S. Mereghetti, in press (astro-ph/0111093).
Kaspi, V. M. & Gavriil, F. P. 2002, IAU Circ., No. 7924
Kaspi, V. M., Gavriil, F. P., Chakrabarty, D., Lackey, J. R., & Muno, M. 2001, ApJ, 558, 253
Kern, B. & Martin, C. 2002, Nature, 417, 527
Landolt, A. U. 1992, AJ, 104, 340
Mereghetti, S. 1995, ApJ, 455, 598
Mereghetti, S., Caraveo, P., & Bignami, G.F. 1992, A& A, 263, 172
Mereghetti, S., Chiarlone, L., Israel, G. L., & Stella, L. 2002, in Neutron Stars, Pulsars and Supernova Remnants, eds. W. Becker, H. Lesch & J. Trümper (Garching: MPE), in press (astro-ph/0205122)
Mereghetti, S., Israel, G. L., & Stella, L. 1998, MNRAS, 296, 689
Monet, D. E. A., et al. 1998, The USNO-A2.0 Catalog (Washington, DC: U.S. Naval Observatory)
Oosterbroek, T., Parmar, A. N., Mereghetti, S., & Israel, G. L. 1998, A&A, 334, 925
Özel, F., Psaltis, D., & Kaspi, V. M. 2001, ApJ, 563, 255
Paul, B., Kawasaki, M., Dotani, T., & Nagase, F. 2000, ApJ, 537, 319
Persson, S. E., Murphy, D. C., Krzeminski, W., Roth, M., & Rieke, M. J. 1998, AJ, 116, 2475
Persson, S. E., Phillips, M., Roth, M., & Birk, C. 2001, "Classic Cam" Near-IR Camera, Users Manual (Las Campanas Observatory, La Serena, Chile)
Persson, S. E., West, S. C., Carr, D. M., Sivaramakrishnan, A., & Murphy, D. C. 1992, PASP, 104, 204
Perna, R., Hernquist, L., & Narayan, R. 2000, ApJ, 541, 344
Rieke, G. H. & Lebofsky, M. J. 1985, ApJ, 288, 618
Seward, F. D., Charles, P. A., & Smale, A. P. 1986, ApJ, 305, 814
Tiengo, A., Göhler, E., Staubert, R., & Mereghetti, S. 2002, A&A, 383, 182
Zombeck, M. V., Chappell, J. H., Kenter, A. T., Moore, R. W., Murray, S. S., Fraser, G. W., & Serio, S. 1995, Proc. SPIE, 2518, 96